Use of GNSS derived ionospheric information to detect and measure Solar Flares

MANUEL HERNÁNDEZ-PAJARES, ALBERTO GARCÍA-RIGO,
ÁNGELA ARAGÓN-ÁNGEL
UPC-IonSAT, Barcelona, Spain (contact e-mail: manuel@ma4.upc.edu)

Recibido: 5/06/2014
Aceptado: 11/10/2014

Abstract
The Ionosphere, the partially ionized atmospheric region ranging from approximately 60 to +1000 km height, is typically affected by spatial and temporal variations, driven by Local Time (solar illumination), Latitude (magnetic field and solar illumination) and time (space weather, among seasonal and solar cycle dependence). It can be indirectly studied from the dual L-band frequency GNSS measurements by assuming the first order ionospheric delay approximation (the higher order ionospheric effects in GNSS typically constitute less than 0.1% of the overall ionospheric effect and only affects very precise applications). Moreover, the Ionosphere is affected as well by ionospheric waves, ,solar flares and other space weather effects. Recent modeling techniques and corresponding results are going to be summarized regarding to the daylight sudden overionization generated by the radiation associated to Solar Flares facing the Earth, and its measurement by means of Global Navigation Satellite Systems. This approach has already been implemented in real-time by the authors.
Key words: Ionosphere, Global Navigation Satellite Systems, Solar Flares.

Uso de información ionosférica obtenida por GNSS para detectar y medir fulguraciones solares

Resumen
La ionosfera, la región atmosférica parcialmente ionizada entre aproximadamente 60 y 1.000 km de altura, está normalmente afectada por las variaciones espaciales y temporales, dependientes de la hora local (iluminación solar), latitud (campo magnético y la iluminación solar) y el tiempo (clima espacial, entre la dependencia del ciclo estacional y solar). Y puede ser estudiada asumiendo la aproximación de primer orden del retardo ionosférico a partir de las mediciones GNSS de frecuencia de banda L duales (los efectos de orden superior suponen menos del 0.1% y únicamente afectan a aplicaciones precisas muy específicas). Sin embargo, la ionosfera puede ser afectada también por otros efectos que no son tan evidentes, como las ondas ionosféricas, y las fulguraciones solares. En este trabajo se resume el modelado y resultados recientes de la sobreionización repentina del hemisferio diurno terrestre, generada por la radiación asociada a erupciones solares que ocurren en el hemisferio solar orientado hacia la Tierra, y medida con sistemas globales de navegación por satélite, como GPS, ya implementado por los autores en un sistema que funciona en tiempo real.
Palabras clave: Ionosfera, Sistemas globales de navegación por satélite, fulguraciones solares.

Referencia normalizada
Hernández-Pajares, M., García-Rigo, A., Aragón-Ángel, A. (2014**).** Use of GNSS derived ionospheric information to detect and measure Solar Flares. *Física de la Tierra*, Vol. 26, 81-87.

Introduction

The Ionosphere can be considered as the region of the Earth atmosphere typically ranging from 50-70 km up to +1000 km, where there is a significant presence of ionized molecules, and free electrons (see Kelley 2009), being this presence high enough to affect space-based and ground-based radiofrequency signals, such as those of the Global Navigation Satellite Systems, GNSS (see for instance in Hernández-Pajares et al. 2011 a review describing the main ionospheric effects on GNSS).

Most part of these free electrons are generated by the continuous and slowly varying EUV solar radiation flux, which is the most geoeffective and responsible, in particular, of the ononization (and heating) of predominant F, and E regions within the Ionosphere (see Kelley 2009). From time to time, some free electrons are suddenly generated by the effect of an unexpected and quick increase of EUV solar radiation flux during solar flares. This phenomena leads to "Sudden Increases in the Total Electron Content" (SITEC, see for instance Smirnov and Smirnova, 2014) , which can be used to issue solar flare warnings (see for example García-Rigo et al. 2007), and to indirectly quantify the fast EUV solar radiation flux variation.

Thanks to dual-frequency GNSS measurements at L-band (about 1.2 GHz and 1.6 GHz for GPS, the American GNSS) such electron content can be monitored with an unprecedented temporal and spatial resolution by means of dozens of MEO transmitters and hundreds of permanent ground receivers. The underlying assumption is to approximate the total ionospheric delay of GNSS signals by its first order approximation, which is directly proportional to the integrated electron density along the ray path (Slant Total Electron Content, STEC) and inversely proportional to the squared frequency. In spite of being a simplification, such assumption is typically accurate at the level of more than 99.9%, where the remaining less than 0.1% is due to the contribution of the higher order terms (see a recent review in Petrie et al. 2011), which are responsible of impeding ultra-precise GNSS applications that require sub-centimeter error level (such as subsidence monitoring, among other applications of GNSS precise coordinates time series –see King et al. 2011–). Details of the impact of the higher order ionospheric terms are provided in the recent comprehensive study Hernández-Pajares et al. 2014.

Other non-usual effects on the ionospheric delay, which have been recently characterized at different latitude regions and solar cycle conditions (see Hernández-Pajares et al. 2012b), are ionospheric waves: The most frequents are the so called Medium Scale Travelling Ionospheric Disturbances (MSTIDs). They follow a climatological pattern, and can significantly degrade GNSS precise positioning services like the Real Time Kinematics (RTK) or Wide Area RTK (see Hernández-Pajares et al. 2000, 2006).

In this paper, it will be briefly summarized how to monitor the generation of the ionospheric free electrons caused by the continuous and slowly varying EUV solar

radiation flux. It will be described how GNSS can provide a useful and accurate way of monitoring solar flares and EUV flux rate by detecting and measuring with GNSS the spatial pattern of the sudden ionospheric overionization, which is associated to the corresponding prompt EUV solar flux increase (basically summarizing the method and results obtained in Hernández-Pajares et al. 2012). Such approach has been already implemented by the authors in real-time in the context of MONITOR project (Prieto-Cerdeira & Béniguel 2011), and thanks to the availability of measurements of the International Real-Time GNSS Service (Caissy et al. 2012).

1. Simple model of solar flare sudden ionospheric overionization and GNSS measurement

Due to the short time scale of the impulsive phase of the solar flares, the associated ionospheric overionization can be approximated by the following simple electron production expression, by neglecting transport terms (see, for example, Hernández-Pajares et al. 2012 and associated references):

$$\frac{\partial V}{\partial t} = \eta' \cdot C(\chi) \cdot \frac{\partial I}{\partial t} \qquad (1)$$

Where V represents the vertically integrated ionospheric free electron density (known as Vertical Total Electron Content, Vertical TEC or VTEC), η' stands for the ionization efficiency, C(χ) represents the cross section for a solar-zenithal angle χ, referred to the value C(0) at the sub-solar point, and ∂I(t)/ ∂t is the sudden solar flux increase at the EUV geoeffective band, at time t.

It is going to be shown that such approximation works very well when it is applied with a simple deprojection factor, cos χ, estimating the slope a(t) (which should be proportional to ∂I(t)/ ∂t) and the independent term b(t). The latter takes into account the geometric consequences of the fact that the overionization occurs at few hundreds of kilometers height and not on the surface.

$$\frac{\partial V}{\partial t} = a(t)\cos\chi + b(t) \qquad (2)$$

To do that, GNSS such as the American Global Positioning System (GPS), offer a unique temporal and spatial resolution and performance to monitor the ionospheric delay. Indeed, taking as basic measurement the difference of dual-frequency L-band carrier phase signals, L1-L2≡LI (which removes any non-frequency dependent terms), a very precise measurement of the STEC is directly obtained, typically better than 0.1 TECU=10^{15} electrons/m^2, but affected by an

ambiguity term that is constant while the GNSS transmitter signal is locked by the receiver (see more details in Hernández-Pajares et al. 2011). Thousands of simultaneous STEC measurements are provided each 30 seconds by the hundreds of permanent receivers of networks e.g. the International GNSS Service (IGS, see for instance Hernández-Pajares et al. 2009) from the GPS satellites in view (typically 5 to 10). In this way, the VTEC rate values needed to solve at each epoch the slope, a(t), and independent term, b(t), of the previous overionization model, can be easily deduced from the consecutive variation of LI (ΔLI) over time (Δt), the deprojection factor from STEC to VTEC (mapping function M), and α=1.05 meters/10 TECU:

$$\frac{\partial V}{\partial t} \approx \frac{\Delta V}{\Delta t} = \frac{1}{M}\frac{\Delta S}{\Delta t} = \frac{1}{\alpha M}\frac{\Delta L_I}{\Delta t} \qquad (3)$$

2. Results

The good performance of the presented overionization model can be seen in Fig.1, where the dependence of VTEC rate, $\partial V/\partial t$, against the cosinus of the solar-zenith angle, $\cos\chi$, behaves linearly at the daylight hemisphere, as expected from previous section.

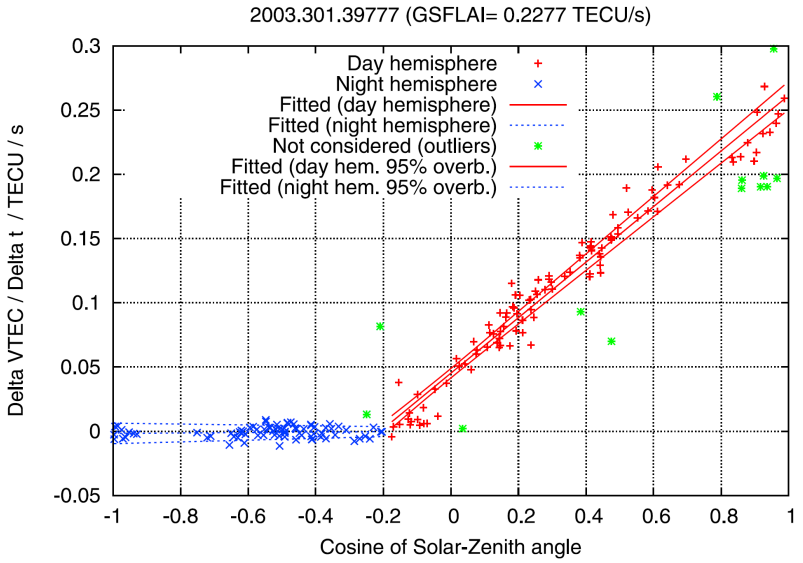

Fig. 1. VTEC rate vs. cosinus of solar-zenith angle, during the second 39777 in GPS time scale, of day 301 of 2003, in the impulsive phase of the X-class solar flare producing the Halloween storm Space Weather event (reproduced from Hernández-Pajares et al. 2012)

Moreover, in Fig. 2, the linear relationship can be appreciated of the slope a(t) (called GNSS Solar Flare Indicator, GSFLAI, and obtained from global GPS measurements looking at the ionospheric overionization spatial pattern), with the EUV solar flux rate, ΔI (directly measured in the EUV band from solar observing satellites), predicted when combining Eq. (1) and (2). The correlation is remarkable, in spite of the different time resolution and completely different observation instrument and environment.

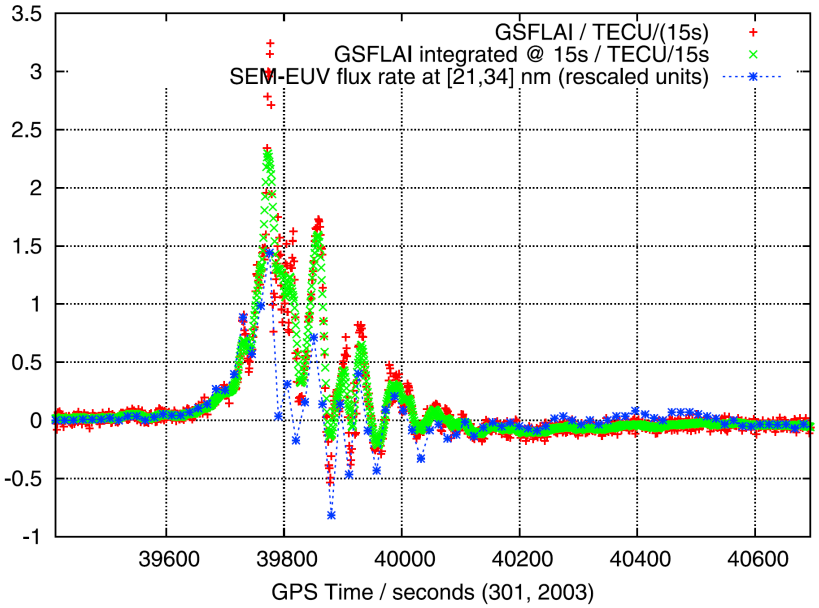

Fig. 2. VTEC rate vs. cosinus of solar-zenith angle, during the second 39777 in GPS time scale, of day 301 of 2003, in the impulsive phase of the X-class solar flare producing the Halloween storm Space Weather event (reproduced from Hernández-Pajares et al. 2012).

Finally, such good relationship has been checked for almost a Solar Cycle, at the limit of the measurement errors for both techniques: the new GNSS-based one, with the direct observation from Space. This can be clearly seen in Fig.3.

3. Conclusions

The influence of solar flares in GNSS measurements has been modelled in such a way that a proxy for the solar EUV rate is obtained (GSFLAI), which compares fairly well with direct measurements from solar observation missions on space (such as the SOHO-SEM instrument). This new solar EUV rate proxy, computed from existing global GNSS networks in real-time, presents some advantages regarding solar observing missions, such as its higher rate and, especially, its immunity to

the relativistic electrons, which interrupt and impede the normal recording of solar flux by spacecraft related instrumentation (see more details in Hernández-Pajares et al. 2012).

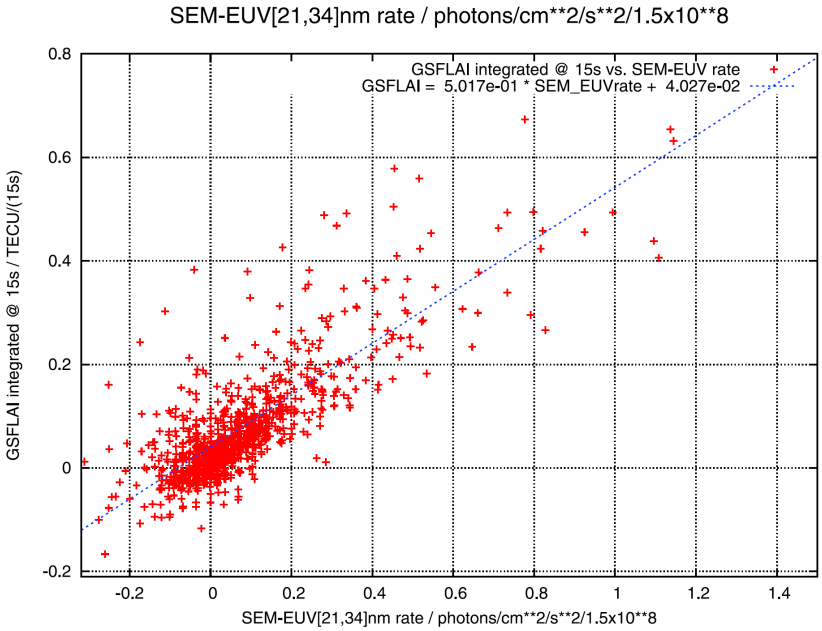

Fig. 3. Zoom of the relationship between the solar EUV flux rate, directly observed by SOHO-SEM instrument at 21-34 nm EUV band, and the GSFLAI value at the same time rate of 15 seconds, obtained from Earth ionospheric overionization pattern measured by GPS at global scale. The data correspond to the days with large scale X-flares, since 2001 to 2011 (the linear fit is also indicated as reference, reproduced from Hernández-Pajares et al. 2012).

Acknowledgments

The authors acknowledge to IGS the availability of the GPS data and satellite products. The technique presented in this work was developed in the context of the authors' participation in the ESA Monitor activity, under a contract of the European Space Agency in the frame of the European GNSS Evolutions Programme.

References

CAISSY, M., AGROTIS, L., WEBER, G., HERNANDEZ-PAJARES, M., & HUGENTOBLER, U. (2012). INNOVATION-Coming Soon-The International GNSS Real-Time Service-, *GPS World*, 23(6), 52.

PRIETO-CERDEIRA, R., & BÉNIGUEL, Y. (2011). The MONITOR project: architecture, data and products. In Ionospheric Effects Symposium, Alexandria VA, May 2011.

GARCÍA-RIGO, A., HERNÁNDEZ-PAJARES, M., JUAN, J. M., & SANZ, J. (2007). Solar flare detection system based on global positioning system data: First results. *Advances in Space Research*, 39(5), 889-895.

HERNÁNDEZ-PAJARES, M., JUAN, J. M., SANZ, J., & COLOMBO, O. L. (2000). Application of ionospheric tomography to real-time GPS carrier-phase ambiguities Resolution, at scales of 400–1000 km and with high geomagnetic activity. *Geophysical Research Letters*, 27(13), 2009-2012.

HERNÁNDEZ-PAJARES, M., JUAN, J. M., & SANZ, J. (2006). Real time MSTIDs modelling and application to improve the precise GPS and GALILEO navigation. *Proceeedings of ION GNSS-2006*, September 2006.

HERNÁNDEZ-PAJARES, M., JUAN, J. M., SANZ, J., ORUS, R., GARCIA-RIGO, A., FELTENS, J. & KRANKOWSKI, A. (2009). The IGS VTEC maps: a reliable source of ionospheric information since 1998. *J Geod.*, 83(3-4), 263-275.

HERNÁNDEZ-PAJARES, M., JUAN, J. M., SANZ, J., ARAGÓN-ÀNGEL, À., GARCÍA-RIGO, A., SALAZAR, D., & ESCUDERO, M. (2011). The ionosphere: effects, GPS modeling and the benefits for space geodetic techniques. *Journal of Geodesy*, 85(12), 887-907.

HERNÁNDEZ-PAJARES, M., GARCÍA-RIGO, A., JUAN, J. M., SANZ, J., MONTE, E., & ARAGÓN-ÀNGEL, A. (2012). GNSS measurement of EUV photons flux rate during strong and mid solar flares. *Space Weather*, 10(12).

HERNÁNDEZ-PAJARES, M., JUAN, J. M., SANZ, J., & ARAGÓN-ÀNGEL, A. (2012b). Propagation of medium scale traveling ionospheric disturbances at different latitudes and solar cycle conditions. *Radio Science*, 47(4).

HERNÁNDEZ-PAJARES, M., ARAGÓN-ÁNGEL, À., DEFRAIGNE, P., BERGEOT, N., PRIETO-CERDEIRA, R., & GARCÍA-RIGO, A. (2014). Distribution and mitigation of higher-order ionospheric effects on precise GNSS processing. *Journal of Geophysical Research*: Solid Earth, 119(4), 3823-3837.

KELLEY, M. C. (2009). The Earth's Ionosphere: Plasma Physics & Electrodynamics (Vol. 96). Academic Press.

KING, M. A., ALTAMIMI, Z., BOEHM, J., BOS, M., DACH, R., ELOSEGUI, P., FUND, F., HERNANDEZ-PAJARES, M., LAVALLEE, D., MENDES-CERVEIRA, P.J., PENNA, N., RIVA, R.E.M., STEIGENBERGER, P., VAN DAM, T., VITTUARI, L., WILLIAMS, S & WILLIS, P. (2010). Improved constraints on models of glacial isostatic adjustment: a review of the contribution of ground-based geodetic observations. *Surveys in geophysics*, 31(5), 465-507.

PETRIE, E. J., HERNÁNDEZ-PAJARES, M., SPALLA, P., MOORE, P., & KING, M. A. (2011). A review of higher order ionospheric refraction effects on dual frequency GPS. *Surveys in Geophysics*, 32(3), 197-253.

SMIRNOV, V. M. AND E. V. SMIRNOVA (2014). Ionospheric Response to the Extreme Solar Burst of October 28, 2003. *Geomagnetism and Aeronomy*, Vol. 54, No. 1, pp. 87[Pleiades Publishing, Ltd.,]